



Published in final edited form as:

*J Am Soc Mass Spectrom.* 2011 August ; 22(8): 1318–1325. doi:10.1007/s13361-011-0135-7.

## Improving Liquid Chromatography-Mass Spectrometry Sensitivity Using a Subambient Pressure Ionization with Nanoelectrospray (SPIN) Interface

Keqi Tang, Jason S. Page, Ioan Marginean, Ryan T. Kelly, and Richard D. Smith

Biological Sciences Division, Pacific Northwest National Laboratory, P.O. Box 999, Richland, WA 99352, USA

### Abstract

In this work, the subambient pressure ionization with nanoelectrospray (SPIN) ion source and interface, which operates at ~15–30 Torr, is demonstrated to be compatible with gradient reversed-phase liquid chromatography-MS applications, exemplified here with the analysis of complex samples (a protein tryptic digest and a whole cell lysate). A low liquid chromatographic flow rate (100–400 nL/min) allowed stable electrospray to be established while avoiding electrical breakdown. Efforts to increase the operating pressure of the SPIN source relative to previously reported designs prevented solvent freezing and enhanced charged cluster/droplet desolvation. A 5- to 12-fold improvement in sensitivity relative to a conventional atmospheric pressure nanoelectrospray ionization (ESI) source was obtained for detected peptides.

### Keywords

ESI; LC-MS; Sensitivity; Subambient pressure ESI; Ion source

### Introduction

Electrospray ionization-mass spectrometry (ESI-MS) [1, 2] is widely applied to a variety of chemical and biological applications due to its broad ability to efficiently create gas-phase ions from solution, and ease of direct coupling with liquid separation techniques [3-5]. The sensitivity of ESI-MS is largely determined by a combination of the effectiveness of producing gas-phase ions from analyte molecules in solution (ionization efficiency) and the ability to transfer the charged species from atmospheric pressure into the low-pressure region of the mass analyzer (transmission efficiency) [6-9]. In spite of the high ESI efficiency, especially at low nL/min flow rates [10-14], large ion losses can occur during transmission from atmospheric pressure to the low pressure region of the mass analyzer [6, 15, 16]. With advances in MS instrumentation, the greatest losses now typically occur at the interface region of the ESI-MS, where a small orifice or a heated capillary inlet (which, e.g., samples only a small portion of the electrospray) leads to significant losses and reduction in achievable instrument sensitivity [6, 9, 11].

An approach we have been developing for eliminating losses associated with the MS inlet involves removing the inlet entirely and placing the ESI source in a lower pressure region [17], where an ion funnel can transmit ions with high efficiency. Electro spraying of

conductive and low volatility liquids at very low pressures was initially developed for space propulsion applications [18], and its implementation as an ion source for mass spectrometry was referred to as electrohydrodynamic ionization (EHD) [19]. This source has proven to be effective with highly nonvolatile liquids at very low flow rates, such as glycerol [19], liquid metals [20, 21], and ionic liquids [22] that prevented the electrospray cone from freezing or boiling by lowering the evaporation rate and allowing sufficient heat transfer at lower pressure. However, these nonvolatile liquids are incompatible with typical liquid-phase separation techniques for routine MS analyses that involve the use of volatile solvents and higher flow rates. An early low-pressure ESI source concept applicable to standard liquid chromatography (LC) solvents described in a 1992 patent [23] involved positioning a metal-coated, tapered electrospray emitter at the entrance of a quadrupole ion guide in a <0.01 Torr chamber, but no results were reported. A later patent by a different group describes a low pressure ESI source at <0.1 Torr followed by a chamber at an elevated pressure to facilitate droplet desolvation and solvated ion declustering [24]. This arrangement was subsequently reported to be capable of detecting 500 ng of caffeine injected onto an LC column [25], but suffered significant losses associated with the need to increase pressure after the ESI source chamber and inefficient declustering/desolvation due to practical limitations on the pressure in that region (i.e., ion losses increase as pressure is increased in order to make declustering/desolvation more efficient). All the ESI sources described in these patents operate electrospray at pressures of <0.1 Torr, far below the pressure range most prone to electrical breakdown (~1 Torr). Regardless, the low ESI operating pressures used in these sources degrade electrospray performance (e.g., due to boiling, freezing, and inefficient evaporation of the solvent), which precluded their practical implementation on ESI-MS.

The subambient pressure ionization with nanoelectrospray (SPIN) ion source and interface has been developed to address difficulties associated with desolvation, ion production, and transmission in a reduced pressure environment [17]. Central to the implementation of the SPIN source is the use of an electrodynamic ion funnel [26] operated in the 15–30 Torr pressure range. The ion funnel is a variation of a stacked ring ion guide [27] created by a series of closely spaced electrodes in which a radio frequency (rf) voltage and a direct current (DC) voltage are applied on each electrode to both confine ions and push ions “drifting” towards the funnel exit. The aperture of the ion guide decreases gradually down to the inner diameter (i.d.) of the conductance-limiting orifice at the exit. The elevated SPIN source operating pressure relative to previous low pressure ESI sources avoids the electrical breakdown at the electrospray onset voltages, and the relatively long residence time in the ion funnel enhances charged cluster/droplet declustering/desolvation, allowing the resulting gas phase ions to be effectively generated and transmitted into the mass spectrometer. In an initial demonstration, the SPIN source has been shown to effectively ionize infused samples using a variety of LC-compatible solvents providing an ~5-fold increase in detection sensitivity compared to a standard heated inlet capillary ESI source and interface design [17]. The previously reported results indicated that ion production efficiency in the SPIN source was similar to the one in atmospheric pressure ESI source, while sample loss due to ion transmission through an inlet was completely eliminated in the SPIN source design.

Although promising, these experiments used the infusion of easily electrosprayed standard solutions with 50% organic solvent (methanol or acetonitrile). Many MS analyses require a liquid-phase separation before MS detection for better dynamic range, selectivity, and sensitivity, and it is crucial to evaluate the SPIN source with a broader range of solvent compositions, such as those commonly encountered with gradient-elution LC separations. Here, we report on coupling gradient reversed-phase LC separations with the SPIN source to separate and analyze complex proteomic samples. Chromatographic and MS peak intensities obtained using the SPIN source at 15–30 Torr and a standard atmospheric pressure ESI source with a typical heated capillary inlet are compared for several peptides. These results

further support the utility of the SPIN source and point the way to ESI source and interface designs approaching ideal MS detection sensitivity.

## Experimental

### Chemicals

Formic acid (FA, Sigma-Aldrich, St. Louis, MO, USA) and trifluoroacetic acid (TFA, Sigma-Aldrich) based LC mobile phases were employed in the experiments reported here. The FA-based mobile phase A consisted of 0.1% FA in purified water (Barnstead Nanopure Infinity System, Dubuque, IA, USA), and mobile phase B consisted of 0.1% FA in acetonitrile (Fisher Scientific, Pittsburgh, PA). The TFA-based mobile phase A consisted of 0.2% acetic acid (Sigma-Aldrich) and 0.05% TFA in purified water, and mobile phase B consisted of 0.1% TFA in 90% acetonitrile and 10% purified water. Tryptic digests of bovine serum albumin [28] (BSA; Pierce Biotechnology, Rockford, IL, USA) and *Shewanella oneidensis* [29] (grown in-house) were prepared using sequencing grade trypsin (Promega, Madison, WI, USA) according to previously reported procedures and the samples were diluted to final concentrations of 0.1  $\mu\text{g}/\mu\text{L}$  and 0.05  $\mu\text{g}/\mu\text{L}$ , respectively.

### HPLC

A Gilson (Middleton, WI, USA) 321 high-performance liquid chromatography (HPLC) system was used to provide an exponential gradient [30] at a flow rate of  $\sim 300$  nL/min for the analysis of the BSA tryptic digest using TFA-based LC mobile phases. An Agilent 1100 Series LC pump (Santa Clara, CA, USA) was used to provide a pre-programmed gradient (minute:percentage of mobile phase B=0:5%, 20:12%, 85:35%, 97:60%, 100:95%) at flow rates between 100–400 nL/min for the analysis of the *Shewanella oneidensis* samples using FA-based LC mobile phases. Reversed-phase capillary LC columns were prepared in-house by slurry packing 3- $\mu\text{m}$  Jupiter C18 stationary phase (Phenomenex, Torrance, CA, USA) into a 60-cm long and 75- $\mu\text{m}$ -i.d./360- $\mu\text{m}$ -o.d. fused silica capillary tubing (Polymicro Technologies, Phoenix, AZ, USA). Sample loading was accomplished using Valco valves (Valco Instruments Co., Houston, TX, USA) with a 5- $\mu\text{L}$  sample loop.

### Electrospray

Electrospray emitters were fabricated by chemically etching sections of either 5- or 10- $\mu\text{m}$ -i.d./150- $\mu\text{m}$ -o.d. fused silica capillary tubing (Polymicro Technologies), as described previously [31]. Hydrophobic treatment of the emitters was accomplished via plasma polymerization and deposition of  $\text{C}_4\text{F}_8$  using a PlasmaLab 100 inductively coupled plasma etch and deposition system (Oxford Instruments, Oxfordshire, UK). The emitters were affixed to a silicon wafer, loaded into the plasma chamber, and exposed to 160 sccm of  $\text{C}_4\text{F}_8$  for 30 s with an ICP power of 2 kW and a frequency of 13.56 MHz. Following this first deposition, the emitter was turned 180° and the procedure was repeated to ensure complete and uniform coating.

A stainless steel union was used to attach the electrospray emitter to the LC column and also served as the connection point for the electrospray voltage (Bertan 205B-03R; Hicksville, NY, USA or Ultravolt Rack X-250, Ronkonkoma, NY, USA). To produce ions at subambient pressure, the emitter was inserted into the vacuum chamber via a vacuum feedthrough as described in detail previously [32]. The conical outlet in the previous design was replaced by a cylindrical outlet, with the emitter protruding  $\sim 2$  mm beyond the cylindrical outlet into the vacuum chamber. This change allowed the emitter tip to be continuously monitored with a Hitachi KP-D20BU video camera (Toyama, Japan) equipped with a long distance microscope (Edmund Optics, Barrington, NJ, USA). In these conditions, the optimum voltage driving the electrospray was  $\sim 6000$  V.

## Mass Spectrometry

Mass spectra were acquired in the 300–2000 $m/z$  range in positive ESI mode with a 0.1 $m/z$  step size on an Agilent MSD1100 (Santa Clara, CA, USA) single quadrupole mass spectrometer equipped with a dual ion funnel interface [33]. The standard atmospheric pressure ESI source used a 7.6 cm long, 490  $\mu\text{m}$  i.d. stainless steel inlet capillary heated at 120 °C and biased 20 V higher than the first ion funnel electrode. The interface chambers hosting ion funnels were respectively pumped by EM28 and EM18 rough pumps (BOC Edwards, Wilmington, MA, USA) down to 15–30 and 1.7 Torr (measured at the pump throat) for each arrangement.

## Results and Discussion

Electrical breakdown and wetting of the ESI emitter outer wall have previously been identified as key reasons for disruption or instability of electrosprays operated at 15–30 Torr [17, 32, 34]. Our initial studies indicated that the SPIN source could be operated without significant challenges when infusing solutions containing 50% organic solvent (methanol or acetonitrile) [17]. Leaking heated CO<sub>2</sub>, an electron scavenger, inside the SPIN source chamber allowed operation at even lower pressures with no electrical breakdown [32]. However, electrospray disruption due to emitter outer wall wetting and liquid beading was still a challenge for the operation over the full range of liquid compositions characteristic to gradient reversed phase LC separations.

The difficulties due to emitter wetting were found to be significantly alleviated by reducing the i.d. of the electrospray emitter from 10 to 5  $\mu\text{m}$ . While the reason for improved performance is not clear, we speculate that the inertia due to increased flow velocity through the smaller emitter minimizes the interaction between the liquid and the solid surfaces. Improved performance was also achieved by coating 10  $\mu\text{m}$  i.d. emitters with a hydrophobic layer, suggesting that interfacial forces at the liquid-solid interface play a significant role in electrospray disruption at decreased pressure. The experiments reported herein were performed on the SPIN source with reversed-phase LC using 5  $\mu\text{m}$  i.d. emitters to enable stable electrospray performance during the entire LC reversed phase gradient.

The *Shewanella oneidensis* tryptic digest sample was first analyzed by LC-ESI-MS, using a small i.d. packed capillary column and a single quadrupole mass spectrometer equipped with a standard heated capillary inlet and an atmospheric pressure ESI source. Measurements were obtained in triplicate for emitter placement and electrospray voltages optimized during infusion experiments. A representative total ion chromatogram (TIC) from one of the analyses is shown as the black trace in Figure 1. The SPIN source was then installed on the same mass spectrometer (by removing the front flange that housed the capillary inlet and replacing it with a flange that contained the SPIN source); all other aspects of the instrument remained unchanged. The same sample was then reanalyzed with the LC-SPIN-MS in triplicate, and one of the resulting TICs is shown as the cyan trace in Figure 1. The insets A and B of Figure 1 are representative mass spectra at the times indicated on the chromatograms.

The most notable difference between the two chromatograms in Figure 1 is the large increase in total ion current with the SPIN source. While these results demonstrated that the SPIN source was able to generate and transmit much larger ion *currents*, such increased currents might not result in corresponding improvements in the *analyte ion* signal as the increased currents could be associated with undetected high  $m/z$  clusters. To confirm the sensitivity increase for analytes, 12 peptides were randomly selected throughout the LC gradient and the corresponding intensities are shown in Figure 2. The LC-SPIN-MS

replicates demonstrate very good reproducibility, while the comparison with the LC-ESI-MS results demonstrates an average 6-fold sensitivity improvement.

The S/N ratios are provided on top of each bar of Figure 2. The S/N ratio is expected to increase with the square root of the signal if only shot noise is present in the experiment. An example is the increase of ~3 times of the S/N ratio for the peptide with  $m/z$  601.4 for an increase of the signal by a factor of ~10. In other cases (e.g., the peptides with  $m/z$  602.8 and 558.7) the S/N ratios do not improve with the same scaling, suggesting S/N is largely defined by 'chemical noise' levels. There are also cases (e.g., the peptides with  $m/z$  1188.2 and 717.2) where the S/N ratio was larger using ESI, and thus suggesting that background species that were not ionized or that were suppressed by the ESI source were contributing to the noise in the SPIN experiments. Certain types of measurements cannot take advantage of an increase in signal unaccompanied by a corresponding increase in the S/N ratio. However, measurements able to exclude or reduce the chemical noise or other interferences (for example MRM measurements) may take full advantage of the larger ion population provided by the SPIN source.

Our previous work using sample infusion indicated that improved SPIN source performance could be obtained at lower flow rates [32]. To test the performance of the SPIN source for a wider range of analytes exhibiting different ionization efficiencies and solvent composition, we performed LC-SPIN-MS measurements at several flow rates, while maintaining the same analysis time and gradient profile. Lower flow rates result in smaller initial droplet sizes and higher charge to analyte ratios that would be expected to provide greater sensitivity. Additionally, the smaller droplet size would further be expected to result in more effective droplet desolvation and potentially large analyte ion currents. Figure 3 shows measured intensities for 12 randomly chosen peptides throughout the LC gradient. By reducing the flow rate from 350 to 200 and 100 nL/min, the average MS peak intensity increased by a factor of 1.7 and 2.4 times clearly showing the merits of operating the SPIN source at lower flow rates.

The present results showing higher signal intensities at lower LC flow rates may seem to contradict the previously published results [17], which indicate lower intensities at decreasing infusion flow rates. However, we need to point out that the flux of analyte delivered to the source in an infusion experiment decreases with the flow rate, which may not always be the case when using a LC separation. Since no significant changes in the widths of the chromatographic peaks were observed in the flow rate range explored by our experiments, the flux of analyte delivered to the ion source was similar under the same column loading conditions. The interplay between the flow rate and the ionization efficiency in the SPIN source was discussed in detail in our previous work [32].

To initially explore the relationship between peptide structure/properties and the observed signal improvement, a less complex sample (BSA digest) was analyzed by both LC-ESI-MS and LC-SPIN-MS. Ten LC-MS peaks were randomly selected, after which the  $m/z$  of the most intense peak in the mass spectrum was recorded for both the standard ESI source and the SPIN interface (Table 1). The charge state of the peak was identified by observing multiple peaks that corresponded to different charge states in the same mass spectrum. A list of peptides commonly detected in a BSA tryptic digest was used to assign the amino acid sequence. A comparison between average peak intensities measured with the two sources (Table 1, last column) shows that the SPIN source increased the sensitivity by ~5- to 12-fold.

With the exception of sensitivity, the standard ESI source and the SPIN source provided similar results. This similarity was observed for each of the  $m/z$  peaks compared between the



two setups in Table 1. For example, Figure 4 shows spectra from the LC-MS analyses using the standard ESI source Figure 4a and the SPIN source Figure 4b. The most intense peak of  $m/z$  494.8 is a +2 charge state peptide with a corresponding +3 charge state detected at  $m/z$  330.3. In addition, a lower intensity peptide is detected at  $m/z$  675.3 with a corresponding +3 charge state at  $m/z$  450.5. An extracted ion chromatogram for the  $m/z$  494.8 peak is also shown in the upper right corner of each spectrum. Both spectra show similar mass profiles with no additional associated peaks (solvent clusters or adducts), which indicates ionization with the SPIN source produced similar analyte ions as an ESI source at atmospheric pressure. The increase in relative intensity for the +3 charge states with the SPIN source may be due to reduced charge loss from proton transfer from the higher charge state, suggesting that the SPIN source may be somewhat gentler than a conventional ESI source and interface.

The range in sensitivity increases (Table 1) is larger than the standard deviations in the analyses suggesting that the gains associated with the SPIN source are not identical for all analytes. In ESI, the fission of droplets that reach the Rayleigh limit preferentially selects (i.e., biases towards) analytes that are on or near the surface of the droplet [35-37]. When aqueous solvents are used, more hydrophobic species tend to be surface active. To determine whether hydrophobicity contributed to the broad range of sensitivity increases, the ratio of peak intensity increase was plotted versus the average hydrophilicity [38] for 20 peptides observed in all LC-MS analyses of BSA digest samples (Figure 5). The plot suggests that the less surface active peptides correlate with more modest increases in intensity, while hydrophobic peptides correlate with the highest increases in intensity. We speculate that this observation may result from observed ions being formed from larger droplets and earlier in the droplet lifetimes when more hydrophobic ions are created, and leaving more hydrophilic analytes trapped in clusters or residual droplets not contributing to detected ions. This observation is consistent with the difference between SPIN source currents and detected ion currents at the LC flow rates used and indicates that there are still substantial ion losses due to incomplete desolvation. If corrected this also suggests that even more significant gain in sensitivity is feasible by improving droplet desolvation (e.g., by increasing the length of the ion funnel drift region or supplying more heat to the interface) and/or the use lower flow rates to further decrease droplet sizes.

## Conclusions

The recently developed SPIN source and interface has been found to efficiently create ions in a 15–30 Torr region of a mass spectrometer and provide effective coupling of LC with MS. The initial evaluation used tryptic digest samples for reversed-phase gradient LC demonstrated that the SPIN source allowed stable nanoelectrospray operation throughout the entire reversed-phase gradient and increased the average instrument sensitivity by a factor of 5-12. The use of an ion funnel in the SPIN source provided effective droplet desolvation and enabled mass spectra similar to a conventional nanoESI source. A lower LC liquid effluent flow rate at an operating pressure of 15–30 Torr improved charged particle desolvation and declustering [39], as smaller droplets facilitated more efficient ion formation. In addition, this pressure regime eliminated solvent freezing, a challenge with previous low pressure ESI sources operated at <0.1 Torr [24]. Thus, the SPIN source can eliminate the major ion losses (shown to be 80%–90% [9]) due to the use of a heated capillary inlet or a small orifice in the conventional ESI-MS instruments and may lead to an ESI-MS platform with optimum ion transmission efficiency from the ion source to the MS detector. Our results also suggest that significant further improvements in sensitivity may be achievable by the use of lower flow rates and conditions that further improve droplet desolvation.

## Acknowledgments

Portions of this research were supported by the NIH National Center for Research Resources (RR018522), the NIH National Cancer Institute (R21 CA126191), and the National Institute of Allergy and Infectious Diseases NIH/DHHS through interagency agreement Y1-AI-4894-01. Experimental portions of this research were performed in the Environmental Molecular Sciences Laboratory, a U.S. Department of Energy (DOE) national scientific user facility located at the Pacific Northwest National Laboratory (PNNL) in Richland, Washington. PNNL is a multiprogram National Laboratory operated by Battelle for the DOE under contract no. DE-AC05-76RLO 1830.

## References

1. Yamashita M, Fenn JB. Electrospray ion source. Another variation on the free-jet theme. *J. Phys. Chem.* 1984; 88:4451–4459.
2. Fenn JB, Mann M, Meng CK, Wong SF, Whitehouse CM. Electrospray ionization-principles and practice. *Mass Spectrom. Rev.* 1990; 9:37–70.
3. Qian WJ, Jacobs JM, Liu T, Camp DG, Smith RD. Advances and challenges in liquid chromatography-mass spectrometry-based proteomics profiling for clinical applications. *Mol. Cell. Proteom.* 2006; 5:1727–1744.
4. Swanson SK, Washburn MP. The continuing evolution of shotgun proteomics. *Drug Discov. Today.* 2005; 10:719–725. [PubMed: 15896685]
5. Shen YF, Smith RD. Advanced nanoscale separations and mass spectrometry for sensitive high-throughput proteomics. *Exp. Rev. Proteom.* 2005; 2:431–447.
6. Kebarle P, Tang L. From ions in solution to ions in the gas phase—The mechanism of electrospray mass spectrometry. *Anal. Chem.* 1993; 65:A972–A986.
7. Schneider BB, Javaheri H, Covey TR. Ion sampling effects under conditions of total solvent consumption. *Rapid Commun. Mass Spectrom.* 2006; 20:1538–1544. [PubMed: 16628560]
8. Cole RB. Some tenets pertaining to electrospray ionization mass spectrometry. *J. Mass Spectrom.* 2000; 35:763–772. [PubMed: 10934430]
9. Page JS, Kelly RT, Tang K, Smith RD. Ionization and transmission efficiency in an electrospray ionization-mass spectrometry interface. *J. Am. Soc. Mass Spectrom.* 2007; 18:1582–1590. [PubMed: 17627841]
10. Wilm MS, Mann M. Electrospray and Taylor-cone theory, Dole's beam of macromolecules at last? *Int. J. Mass Spectrom. Ion Processes.* 1994; 136:167–180.
11. Wilm M, Mann M. Analytical properties of the nanoelectrospray ion source. *Anal. Chem.* 1996; 68:1–8. [PubMed: 8779426]
12. Valaskovic GA, Kelleher NL, McLafferty FW. Attomole protein characterization by capillary electrophoresis-mass spectrometry. *Science.* 1996; 273:1199–1202. [PubMed: 8703047]
13. Smith RD, Shen Y, Tang K. Ultrasensitive and quantitative analyses from combined separations-mass spectrometry for the characterization of proteomes. *Acc. Chem. Res.* 2004; 37:269–278. [PubMed: 15096064]
14. El-Faramawy A, Siu KWM, Thomson BA. Efficiency of nanoelectrospray ionization. *J. Am. Soc. Mass Spectrom.* 2005; 16:1702–1707. [PubMed: 16095913]
15. Smith RD, Loo JA, Edmonds CG, Barinaga CJ, Udseth HR. New developments in biochemical mass spectrometry: electrospray ionization. *Anal. Chem.* 1990; 62:882–899. [PubMed: 2194402]
16. Cech NB, Enke CG. Practical implications of some recent studies in electrospray ionization fundamentals. *Mass Spectrom. Rev.* 2001; 20:362–387. [PubMed: 11997944]
17. Page JS, Tang K, Kelly RT, Smith RD. Subambient pressure ionization with nanoelectrospray source and interface for improved sensitivity in mass spectrometry. *Anal. Chem.* 2008; 80:1800–1805. [PubMed: 18237189]
18. Hogan JJ, Carson RS, Schneider JM, Hendricks CD. Factors influencing electrically sprayed liquids. *AIAA J.* 1964; 2:1460–1461.
19. Cook KD. Electrohydrodynamic mass-spectrometry. *Mass Spectrom. Rev.* 1986; 5:467–519.
20. Prewett, PD.; Mair, GLR. *Focused Ion Beams from LMIS.* Research Study Press; Somerset: 1991.

21. Gamero-Castano M, Aguirre-de-Carcer I, de Juan L, e la Mora JF. On the current emitted by Taylor Cone-Jets of electrolytes in Vacuo—implications for liquid metal ion sources. *J. Appl. Phys.* 1998; 83:2428–2434.
22. Romero-Sanz I, de la Mora JF. Energy distribution and spatial structure of electrosprays of ionic liquids in vacuo. *J. Appl. Phys.* 2004; 95:2123–2129.
23. Jorgenson, JW.; Dohmeier, DM. Patent No. 5,115, 131. 1992.
24. Sheehan, EW. Patent No. 5,838,002. 1998.
25. Sheehan, EW.; Willoughby, RC.; Jarrell, JA.; Strand, DM. USA Patent No. 6,278,111. 2001.
26. Kelly RT, Tolmachev AV, Page JS, Tang KQ, Smith RD. The ion funnel: theory, implementations, and applications. *Mass Spectrom. Rev.* 2010; 28:294–312. [PubMed: 19391099]
27. Gerlich, D. State-selected and state-to-state ion–molecule reaction dynamics. Part 1. Experiment. In: Ng, CY.; Baer, M., editors. *State-Selected and State-to-State Ion–Molecule Reaction Dynamics*. Wiley; New York: 1992. p. 1-76.
28. Kinter, MM.; Sherman, NE. *Protein Sequencing and Identification Using Tandem Mass Spectrometry*. Wiley-Interscience; New York: 2000.
29. Shen YF, Zhang R, Moore RJ, Kim J, Metz TO, Hixson KK, Zhao R, Livesay EA, Udseth HR, Smith RD. Automated 20 kpsi RPLC-MS and MS/MS with chromatographic peak capacities of 1000–1500 and capabilities in proteomics and metabolomics. *Anal. Chem.* 2005; 77:3090–3100. [PubMed: 15889897]
30. Shen YF, Zhao R, Belov ME, Conrads TP, Anderson GA, Tang KQ, Pasa-Tolic L, Veenstra TD, Lipton MS, Udseth HR, Smith RD. Packed capillary reversed-phase liquid chromatography with high-performance electrospray ionization Fourier transform ion cyclotron resonance mass spectrometry for proteomics. *Anal. Chem.* 2001; 73:1766–1775. [PubMed: 11338590]
31. Kelly RT, Page JS, Luo Q, Moore RJ, Orton DJ, Tang K, Smith RD. Chemically etched open tubular and monolithic emitters for nanoelectrospray ionization mass spectrometry. *Anal. Chem.* 2006; 78:7796–7801. [PubMed: 17105173]
32. Marginean I, Page J, Tolmachev A, Tang K, Smith RD. Achieving 50% ionization efficiency in subambient pressure ionization with nanoelectrospray. *Anal. Chem.* 2010; 82:9344–9349. [PubMed: 21028835]
33. Ibrahim Y, Tang K, Tolmachev AV, Shvartsburg AA, Smith RD. Improving mass spectrometer sensitivity using a high-pressure electrodynamic ion funnel interface. *J. Am. Soc. Mass Spectrom.* 2006; 17:1299–1305. [PubMed: 16839773]
34. Marginean I, Page JS, Kelly RT, Tang KQ, Smith RD. Effect of pressure on electrospray characteristics. *Appl. Phys. Lett.* 2009; 95:184103. [PubMed: 19997584]
35. Enke CG. A predictive model for matrix and analyte effects in electrospray ionization of singly-charged ionic analytes. *Anal. Chem.* 1997; 69:4885–4893. [PubMed: 9406535]
36. Tang K, Smith RD. Physical/chemical separations in the break-up of highly charged droplets from electrosprays. *J. Am. Soc. Mass Spectrom.* 2001; 12:343–347. [PubMed: 11281610]
37. Schmidt A, Karas M, Dülcks T. Effect of different solution flow rates on analyte ion signals in nano-ESI MS, or when does ESI turn into Nano-ESI? *J. Am. Soc. Mass Spectrom.* 2003; 14:492–500. [PubMed: 12745218]
38. Hopp TP, Woods KR. Prediction of protein antigenic determinants from amino-acid-sequences. *Proc. Natl. Acad. Sci. U. S. A.* 1981; 78:3824–3828. [PubMed: 6167991]
39. Thomson BA. Declustering and fragmentation of protein ions from an electrospray ion source. *J. Am. Soc. Mass Spectrom.* 1997; 8:1053–1058.



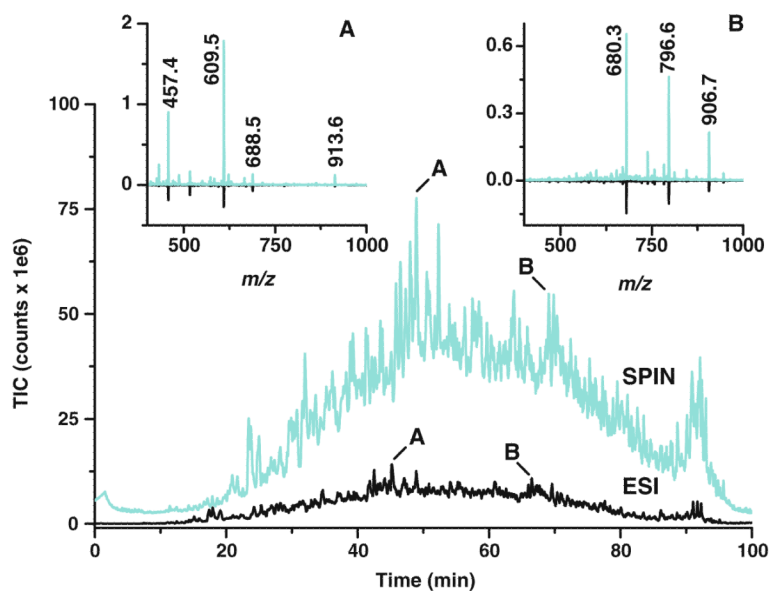


**Figure 1.** TICs for the LC-MS analysis of 0.5 µg tryptic digest of *Shewanella oneidensis* with a standard atmospheric pressure ESI source (black trace) and the SPIN source (cyan trace) and representative mass spectra at the times indicated on the chromatograms (insets A and B)

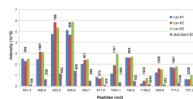


**Figure 2.** Intensities corresponding to 12 peptides randomly chosen throughout the gradient in three consecutive LC-SPIN-MS experiments compared with intensities measured in an LC-ESI-MS experiment. Numbers on top of each bar represent the S/N ratios with average S/N ratios provided for LC-SPIN-MS experiments

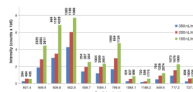


**Figure 3.** Intensities corresponding to 12 peptides randomly chosen throughout the gradient in consecutive LC-SPIN-MS experiments as a function of flow rate. Numbers on top of each bar represent the S/N ratios

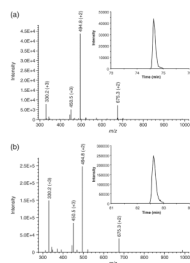


**Figure 4.** Extracted ion chromatogram for  $m/z$  494.8 and corresponding mass spectra for the standard ESI source (a) and the SPIN source (b)

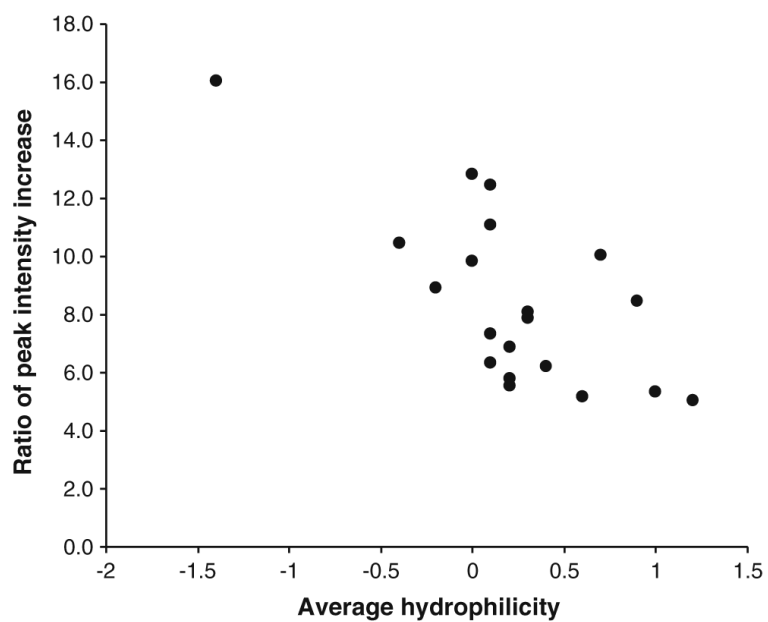


**Figure 5.** Ratio of the peak intensity increases versus the calculated average hydrophilicity for peptides from the analysis of the BSA tryptic digest sample by the standard ESI source and the SPIN source



Ten Randomly Selected LC-MS Peptide Peaks from the Analysis of 0.5  $\mu$ g BSA Tryptic Digest Sample with a Standard Atmospheric ESI Source and the SPIN Source and Interface

**Table 1**

<i>m/z</i>	Charge state	Detected peptide		Conventional ESI source		SPIN source		Intensity ratio
		Sequence	Sequence	Average intensity	% st. dev.	Average intensity	% st. dev.	
395.2	2	LVTDLTK	LVTDLTK	6240013.9	800000	23.9	12.8	12.8
424.2	2	LSQKFPK	LSQKFPK	52600	12.9	414000	16.5	7.9
464.3	2	YLYEIAK	YLYEIAK	47400	14.5	495000	19.1	10.5
480.7	3	RHPEYAVSVLLR	RHPEYAVSVLLR	49400	23.8	486000	3.5	9.8
494.8	2	TPVSEKVTK	TPVSEKVTK	37200	19.0	193000	24.7	5.2
507.9	2	QTALVELLK	QTALVELLK	33800	6.1	302000	8.7	8.9
547.5	3	KVPQVSTPTLVEVSR	KVPQVSTPTLVEVSR	58700	12.1	650000	10.3	11.1
571.9	2	KQTALVELLK	KQTALVELLK	43700	7.1	277000	10.3	6.3
655.3	3	LKPDPNTLCDEFKADEK	LKPDPNTLCDEFKADEK	16000	19.2	85000	11.7	5.3
735.7	4	AFDEKLFTHADICITLPDTEKQIKK	AFDEKLFTHADICITLPDTEKQIKK	13900	30.0	86800	8.1	6.2